Synthesis and Properties of Iron(II) and Manganese(II) Complexes Derived from a Topologically Constrained Pentadentate Ligand

Simon Collinson,[†] Nathaniel W. Alcock,[‡] Ahasuya Raghunathan,[§] Pawan K. Kahol,[§] and Daryle H. Busch*[,†]

Chemistry Departments, University of Kansas, Lawrence, Kansas 66045, University of Warwick, Coventry CV4 7AL, U.K., and Wichita State University, Wichita, KS 67260

Received December 9, 1998

The novel bicyclic pentadentate ligand 5-methyl-1,5,9,24,25-pentaazapentacyclo[7.7.7.5.5]pentacosane-11,13,15,18(25),20,22-hexene (L_1) has been synthesized. Because of its cross-bridged topology it exhibits a relatively rigid *preorganized* conformation especially appropriate to complex formation, as shown by the crystal structure of the monoprotonated ligand salt, HL_1ClH_2O [orthorhombic, $P2_12_12_1$, $a = 9.4405(5)$ Å, $b = 13.3617(5)$ Å, $c = 16.710(1)$ Å]. The complexes of L_1 with both iron(II) and manganese(II) have been characterized, including the crystal structures of $[FeL_1CH_3CN][FeCL_4]$ and $[MnL_1Cl][PF_6]$ [monoclinic, $P2_1/n$, $a = 10.0460(5)$ Å, $b = 19.237(9)$ Å, $c = 15.6254(8)$ Å, $\beta = 95.97(2)°$ and $a = 7.745(2)$ Å, $b = 22.786(4)$ Å, $c = 14.639(4)$ Å, $\beta = 105.074(10)°$ respectively]. The manganese complex is high spin with $\mu_{eff} = 5.96$ and $\theta = 2.5 \pm 0.8$ cm^{-1}, indicating weak ferromagnetic interactions. The reactions of the complexes with *tert*-butyl hydroperoxide and hydrogen peroxide have been shown by ESR spectroscopy to produce the *tert*-butyl peroxyl and hydroperoxyl radicals, as evidenced by their spin adducts with the spin traps *N*,*N*-dimethyl-1-pyrroline-*N*-oxide and *N*-*tert*-butyl−phenyl-nitrone.

Introduction

The effects of increasing topological and flexibility constraints on ligands[1] has been a subject of recent interest in macrocyclic[2] chemistry, particularly in relation to potential improvement in complex stability.[3] The incorporation of intramolecular bridges spanning nonadjacent nitrogen atoms (cross-bridging) in tetraaza-macrocycles[4] produces metal complexes with structures and properties that may be described as intermediate between simple aza-macrocycles and cryptands, such as Sargeson's hexadentate cages.[5] For this reason, the synthesis of rigid intramolecularly bridged aza-macrocycles has been the subject of considerable current research.[3,4] However, the metal ion coordination chemistry of these important ligands has developed only slowly,[6] in part because the highly basic, *proton sponge* nature of the ligands favors their interaction with protons in preference to metal ions.

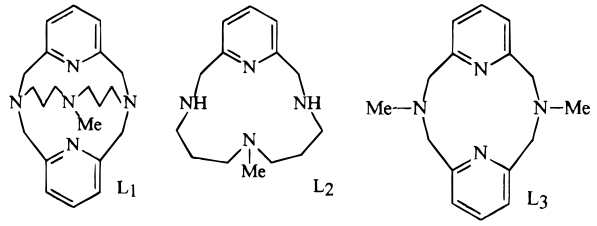

Figure 1. Ligands described in text.

The present paper reports a novel cross-bridged ligand (L_1 in Figure 1) which demonstrates a high degree of preorganization[2] with respect to metal complexation. To synthesize complexes between ligands that are proton sponges and highly hydrolyzable metal ions that are easily transformed into inert mineral forms, it is necessary to avoid both protonic solvents and oxygen. In this way, the formation of complexes of L_1 with iron(II) and manganese(II) ions has been achieved and the properties of these complexes have been determined.

[†] University of Kansas.
[‡] University of Warwick.
[§] Wichita State University.

(1) (a) Busch, D. H. *Chem. Rev.* **1993**, *93*, 847. (b) Busch, D. H. *The Compleat Coordination Chemistry—What a Difference a Century Makes*; Werner Centennial Volume, ACS Symposium Series 565; American Chemical Society: Washington, DC, 1994; pp 148−164. (c) Busch, D. H. Ligand Design for Enhanced Molecular Organization—Selectivity and Specific Sequencing in Multiple Receptor Ligands, and Orderly Molecular Entanglements. In *Transition Metal Ions in Supramolecular Chemistry*; Fabbrizzi, L., Ed.; Kluwer: Dordrecht, 1994; pp 55−79.

(2) (a) Cabbiness, D. K.; Margerum, D. W. *J. Am. Chem. Soc.* **1969**, *91*, 6540. (b) Busch, D. H. *Acc. Chem. Res.* **1978**, *11*, 392. (c) Lindoy, L. F. *The Chemistry of Macrocyclic Ligand Complexes*; Cambridge University Press: Cambridge, 1989. (d) Cram, D. J.; deGrandpe, M. P.; Knobler, C. B.; Truebold, K. N. *J. Am. Chem. Soc.* **1984**, *106*, 3286.

(3) Hubin, T. J.; McCormick, J. M.; Collinson, S. R.; Alcock, N. W.; Busch, D. H. *Chem. Commun. (Cambridge)* **1998**, 1675.

(4) (a) Weisman, G. R.; Rogers, M. E.; Wong, E. H.; Jasinski, J. P.; Paight, E. S. *J. Am. Chem. Soc.* **1990**, *112*, 8604. (b) Ciampolini, M.: Nardi, N.; Voltaconi, B.; Micheloni, M. *Coord. Chem. Rev.* **1992**, *120*, 223. (c) Weisman, G. R.; Wong, E. H.; Hill, D. C.; Rogers, M. E.; Reed, D. P.; Calabrese, J. C. *Chem. Commun. (Cambridge)* **1996**, 947.

(5) (a) Creaser, I. I.; Harrowfiels, J. M.; Herlt, A. J.; Sargeson, A. M.; Geue, R. J.; Snow, M. R. *J. Am. Chem. Soc.* **1977**, *99*, 3181. (b) Sargeson, A. M. *Chem. Br.* **1979**, *15*, 23. (c) Sargeson, A. M. *Pure Appl. Chem.* **1984**, *56*, 1603. (d) Alpha, B.; Anklam, B.; Deshenaux, R.; Lehn, J.-M.; Pietraskiewicz, M. *Helv. Chim. Acta* **1988**, *71*, 1042.

(6) (a) Ramasubbu, A.; Wainwright, K. P. *J. Chem. Soc., Chem. Commun.* **1982**, 277. (b) Ciampolini, M.; Micheloni, M.; Vizza, F.; Zanobini, F.; Chimichi, S.; Dapporto, P. *J. Chem Soc., Dalton Trans.* **1986**, 505. (c) Hancock, R. D.; Dobson, S. M.; Evers, A.; Wade, P. W.; Ngwenya, M. P.; Boeyens, J. C. A.; Wainwright, K. P. *J. Am. Chem. Soc.* **1988**, *110*, 2788. (d) Bencini, A.; Bianchi, A.; Borselli, A.; Ciampolini, M.; Garcia-Espana, E.; Dapporto, P.; Micheloni, M.; Paoli, D.; Ramirez, J. A.; Valtancoli, *B. Inorg. Chem.* **1989**, *28*, 4279.(e) Krakowiak, K. E.; Bradshaw, J. S.; Kou, X.; Dally, N. K. *Tetrahedron* **1995**, *51*, 1599. (f) Bazzicalupi, C.; Bencini, A.; Bianchi, A.; Fusi, V.; Paoli, D.; Ramirez, J. A.; Valtancoli, B.; Golub, G.; Cohen, H.; Meyerstein, D. *J. Chem. Soc, Dalton Trans.* **1995**, 2377.

10.1021/ic981410f CCC: $19.00
Published on Web 01/28/2000

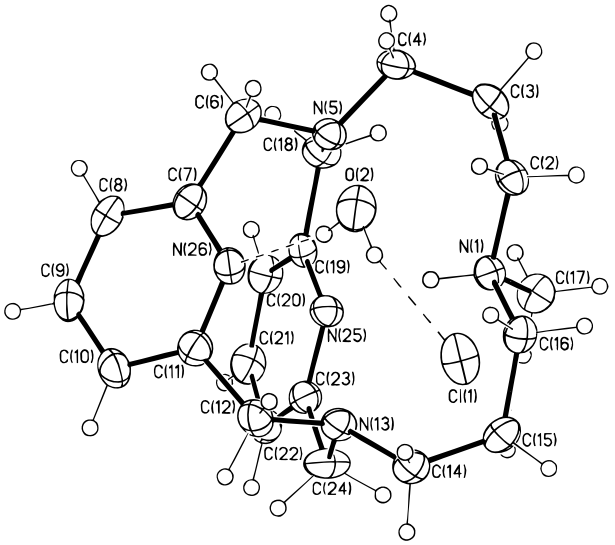

Figure 2. Structure of HL_1ClH_2O, showing the hydrogen bonds.

Results and Discussion

Ligand Synthesis. The macrocycle 7-methyl-3,7,11,17-tetraazabicyclo[11.3.1]heptadecane-1(17),13,15-triene was successfully cross-bridged intramolecularly using O,O′-bis(methanesulfonate)-2,6-pyridine dimethanol, under high dilution conditions. The highest yields were obtained in the presence of sodium carbonate. Potassium carbonate proved less effective, and, with lithium carbonate, the product proved to be a mixture of the metal-free ligand and its lithium complex; the mass spectrum showed peaks at 352 (HL_1^+) and 358 (LiL_1^+). The ^{1}H NMR spectrum (CD_3CN) supported the presence of two species, but the pure lithium complex could not be obtained by recrystallization.

The ligand L_1 has been structurally characterized as its hydrochloride monohydrate (Figure 2). Ready protonation of this ligand is not surprising considering the extensive studies by Weisman and Ciampolini and their co-workers on similar cross-bridged tetraaza-macrobicycles.[4] Ciampolini's related pentadentate ligands, derived from cyclen, were all found to be strongly basic in nature. The presence of the chloride anion was unexpected since no chloride- or chlorine-containing species were used in the later stages of the synthesis. Likely chloride sources are the methanesulfonyl chloride used in ligand synthesis and the alumina column used in purification. Earlier attempts to obtain ligand salts suitable for crystal structure determination yielded only poorly crystalline di- and triprotonated ligand salts.

The X-ray structure of the related ligand 2,11-diaza[3,3](2,6)-pyridinophane (L_3 in Figure 1) shows that the nonaromatic tertiary amine nitrogens adopt a conformation with their lone pairs orientated out of the macrocyclic cavity,[7] suggesting that the conformation of the ligand in its metal complexes may not represent the favored energy minimum. That is, there may be a conformational cost when the ligand binds to a metal ion.[8] In contrast, it can clearly be seen from the X-ray structure of the ligand salt HL_1ClH_2O that the amine lone pairs point toward the ligand cavity demonstrating a higher degree of preorganization with respect to complexation. The solvent water is hydrogen bonded both to one of the pyridine nitrogen atoms (O(2)···N(26) 2.877(2) Å) and to the chloride anion (O(2)···Cl(1) 3.244(2) Å).

The ^{1}H NMR (CD_3CN) (Figure 3a) of the ligand supports the view that the ligand has a relatively rigid conformation in solution. Although the protons of the two pyridine rings are not distinguishable, the methylenic protons adjacent to the pyridine ring are clearly split into an AB pattern. This splitting arises because these protons are positioned either between the two pyridine rings or near the alkyl bridge. In contrast, the related ligand lacking an intramolecular bridge, L_3, only exhibits this kind of splitting on cooling to −60 °C (in deuteriomethanol).[7] Therefore the introduction of the intramolecular bridge in L_1 appears to lock the ligand into a conformation appropriate for metal coordination. As indicated earlier,[8] this introduces a barrier to complexation, but the positive consequence of this locked structure is that it produces an even greater barrier to metal ion dissociation once the complex has been formed. Thus the complexes of L_1 are expected to enjoy both kinetic and thermodynamic stability.

Formation and Characterization of Complexes. Initial attempts at complexing L_1 with hydrated metal salts yielded compounds analyzing as diprotonated ligand salts. In the case of manganese, a black powder was also deposited during these reactions. It has long been known that difficulties may arise when trying to synthesize iron(II) complexes with macrocyclic amine ligands because of the tendency of the iron(II) ions to form hydroxy species which are easily oxidized to iron(III) derivatives in the presence of only trace amounts of water and/or air.[9] In successful complexation studies anhydrous metal salts were employed in proton-free media.

When L_1 reacts with hexakis(acetonitrile)iron(II) trifluoromethanesulfonate in acetonitrile, a dark red oily solid is produced. The dominant peak at 442 in the mass spectrum of the red oil corresponds to $Fe(L_1)Cl^+$, again showing the unexpected presence of halide. Recrystallization from ethanol afforded crystals suitable for X-ray crystallography. The X-ray structure (below) shows that the recrystallized complex has the formula $[Fe(L_1)MeCN]^{2+}[FeCl_4]^{2-}$ including a coordinated acetonitrile molecule and a tetrachloroferrate(II) anion. Similarly, reaction of the ligand with bis(pyridine)iron(II) chloride also yielded a dark red solid. The mass spectrum again showed the FeL_1Cl^+ peak at 442, but a satisfactory analysis could not be obtained. The sharp ^{1}H NMR spectrum indicates that the complex is low spin. Attempts at metathesis of the noncoordinating anion with either hexafluorophosphate or tetrafluoroborate failed to yield a pure complex.

Reaction of bis(pyridine)iron(II) chloride with L_1, sodium tetrafluoroborate, and triethylamine in acetonitrile yielded a product having the formulation $[FeL_1(H_2O)](BF_4)_2$. Conductivity measurements confirm the formulation as a 1:2 electrolyte in acetonitrile (238 Ω^{-1} cm^2 mol^{-1}), although in water the value was slightly below the expected value (205 Ω^{-1} cm^2 mol^{-1}).

Metathesis of the complex formed from iron trifluoromethanesulfonate with the strong field thiocyanate anion gives a red solid having the composition $FeL_1(SCN)_2$. This compound

(7) Kruger, H. J. *Chem. Ber.* **1995**, *128*, 531.

(8) It is commonly assumed that the necessity for changing the conformation of a ligand in order to form a metal complex will make it difficult to bind the ligand. This is a fallacy. Interchanging conformations is an essential part of the process of binding a complicated ligand to a metal ion, so that flexibility actually makes complexing easier in the mechanistic sense. Since bonds to metal ions are essentially always formed or broken one at a time and since almost all solution reactions involve metal ions that are already bound to other ligands (solvent, counterions, etc.), perfect preorganization of a complicated ligand so that it is ideally complementary to a metal ion constitutes a major kinetic barrier to binding. It is necessary for that perfectly preorganized ligand to rearrange itself so that the first, second, etc. bond to the metal ion can be formed. This is why the rates of binding decrease in the order monodentate ligand, flexible linear chelate > macrocycle > cryptate, for example.

(9) Goedken, V. L.; Busch, D. H. *J. Am. Chem. Soc.* **1972**, *94*, 7355.

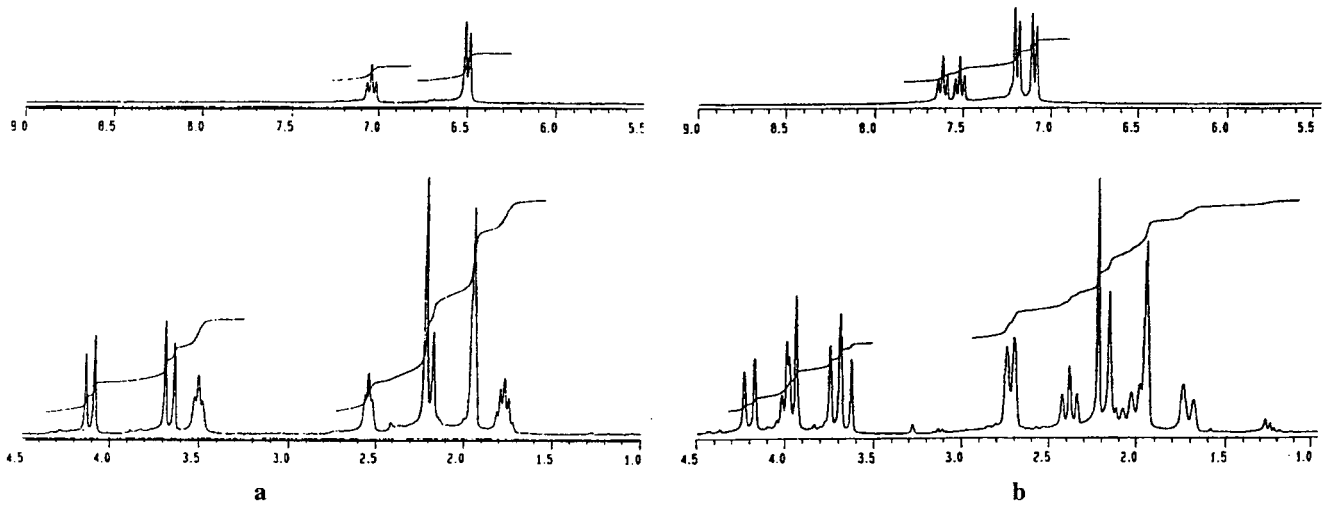

Figure 3. ^{1}H NMR spectra (CD_3CN, 300 MHz): (a) ligand L_1; (b) $FeL_1(SCN)_2$.

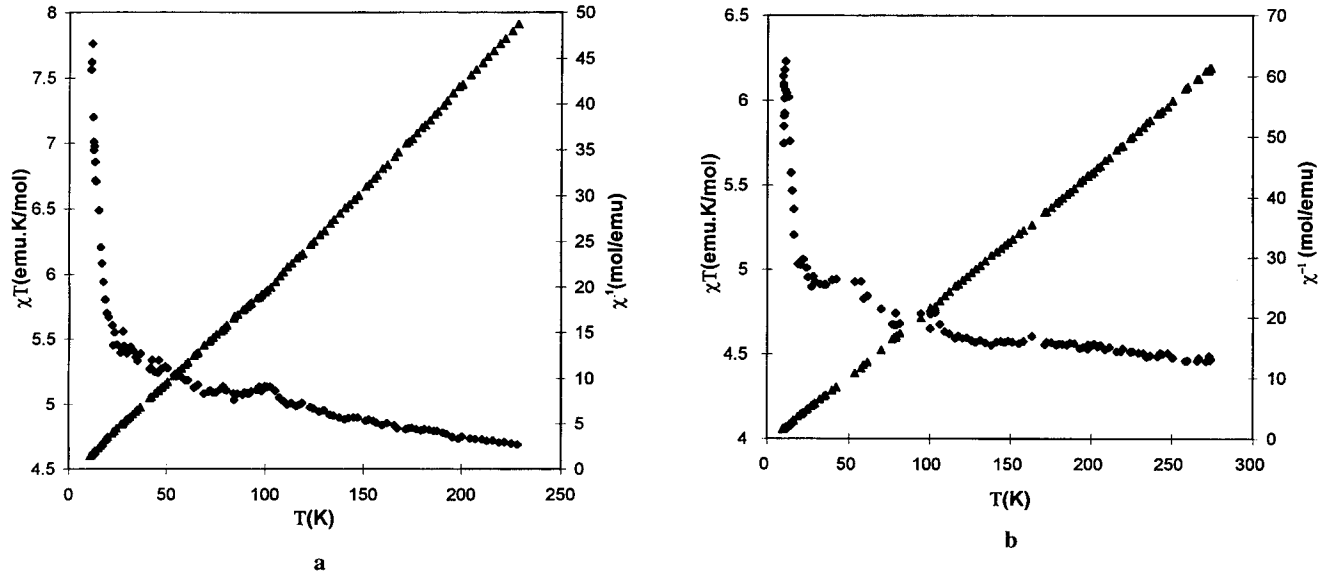

Figure 4. Cryomagnetic data for (a) $Mn(L_1)Cl(PF_6)$ and (b) $MnL_1(CF_3SO_3)_2$.

exhibits a mass spectral peak for FeL_1SCN^+ at 465 and the sharp ^{1}H NMR (Figure 3b); both observations attribute a low spin electronic structure to the iron(II) ion and support pentadentate ligand binding as was found in the X-ray crystal structure of $[FeL_1(CH_3CN)](FeCl_4)$. Two distinct sets of pyridine resonances are displayed and two different AB patterns are seen for the methylenic protons adjacent to the pyridine rings. The IR spectrum shows two thiocyanate bands and is consistent with one bound and one free counterion. Correspondingly, the complex was shown to be a 1:1 electrolyte in water (123 Ω^{-1} cm^2 mol^{-1}), while in acetonitrile solution the conductance value was slightly lower than expected for a 1:1 electrolyte (92 Ω^{-1} cm^2 mol^{-1}).

For manganese(II), complexation was first attempted with bis(pyridine)manganese(II) chloride. The first product from this reaction was a white powder which analyzed as $H_2L_1(MnCl_4)$ (Calcd: C, 45.98; H, 5.70; N, 12.77. Found: C, 45.50; H, 5.15; N, 13.10), but a second crop of crystals proved to be the orange complex $[MnL_1Cl]_2(MnCl_4)$. This could be metathesized with hexafluorophosphate anions during or after formation to yield the complex salt $[MnL_1Cl](PF_6)$. The latter compound is especially important because the presence of only one type of manganese within the complex greatly facilitates characterization. The structure of this complex was determined by X-ray crystallography (below). A higher yield synthesis of $MnL_1(CF_3SO_3)_2$ was developed starting with manganese(II) trifluoromethanesulfonate. Both manganese(II) compounds were determined to be high spin in solution by the Evans method; for $MnL_1Cl(PF_6)$, $\mu_{eff} = 5.96$, and for $MnL_1(CF_3SO_3)_2$, $\mu_{eff} = 5.77$.

The magnetic susceptibilities of the solid manganese compounds were studied over the temperature range 5−295 K using a force magnetometer. The experimental data are graphed in the forms χT versus T and $1/\chi$ versus T in Figure 4 (a, $[MnL_1Cl](PF_6)$; b, $MnL_1(CF_3SO_3)_2$). The observed linear dependence of $1/\chi$ on temperature, in combination with the crystal structure, suggests that the data can be fitted to the equation

$$\chi = N\mu_{eff}^2/3k_B(T - \theta)$$

where χ is expressed per mole of manganese ions and θ is a Weiss constant to correct for the presence of neighboring manganese interactions. A linear regression of the $1/\chi$ versus T data yields the values $\mu_{eff} = 5.97$, $\theta = 3.8 \pm 1.3$ cm^{-1} for $[MnL_1Cl](PF_6)$, and $\mu_{eff} = 5.96$, $\theta = 2.5 \pm 0.8$ cm^{-1} for $MnL_1(CF_3SO_3)_2$. The fitted parameters μ_{eff} and θ clearly indicate

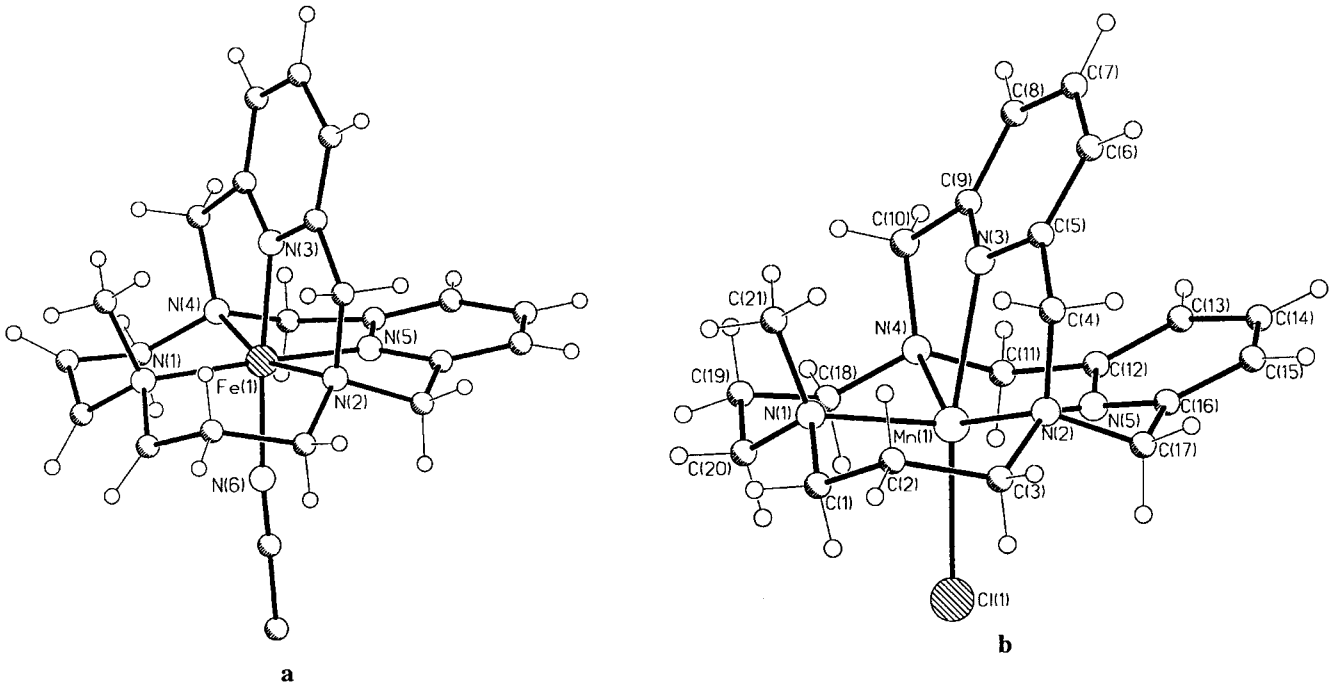

Figure 5. X-ray crystal structures: (a) the cation of $[FeL_1(CH_3CN)][FeCl_4]$; (b) the cation of $[MnL_1Cl][PF_6]$.

the presence of weak ferromagnetic interactions between manganese ions.

In acetonitrile $[MnL_1Cl](PF_6)$ is a 1:1 electrolyte (147 Ω^{-1} cm^2 mol^{-1}) and $MnL_1(CF_3SO_3)_2$ is a 1:2 electrolyte (271 Ω^{-1} cm^2 mol^{-1}). However, in water both complexes give values intermediate between a 1:1 and a 1:2 electrolyte, i.e., $[MnL_1Cl](PF_6)$, 184 Ω^{-1} cm^2 mol^{-1}, and $MnL_1(CF_3SO_3)_2$, 188 Ω^{-1} cm^2 mol^{-1}, indicating that there is some association of the anion at the sixth coordination site.

The stabilities of these complexes with respect to dissociation of the pentadentate ligand were demonstrated by dissolving $MnL_1(CF_3SO_3)_2$ in 0.1 M HNO_3 to yield an orange solution, whose UV spectrum remains unchanged for more than 2 weeks. The stability of the complex is somewhat lower in 0.1 M potassium hydroxide, where a precipitate formed after about 2 h. In earlier studies, manganese(II) complexes with tetraaza-macrocycles have been reported to be unstable at extreme pH values in aqueous solution, decomposing immediately.[10]

Attempts to prepare solutions of $[Fe(L_1)SCN]SCN$ in 0.1 M HNO_3 were hindered by the slow rate of dissolution of the complex, combined with the propensity of the iron to undergo oxidation in the presence of acid.[11] Accordingly the HNO_3 solution attained a deep blue color ($\lambda_{max} = 584$ nm, $\epsilon = 1386$ M^{-1} cm^{-1}) suggesting that oxidation had occurred. Once formed, however, the iron(III) complex appeared to be stable in acid solution.

X-ray Crystal Structures. Both crystal structures of L_1 complexes contain the metal ions in pseudo-octahedral coordination geometries, displaying the expected pentadentate ligand binding and with the coordination sphere completed by an acetonitrile (Fe) or a chloride (Mn) (Figure 5a,b). Table 1 provides comparative dimensions for the two structures. In the structure of the iron complex, the Fe to N(py) distances are somewhat shorter than those to N(sp) and N(sp^3) (means: 1.897, 1.942, and 2.073 Å, respectively). All of these distances are rather longer than those reported[12] for the same N-centers in a similar low spin iron(II) complex; this lengthening is probably a consequence of the ligand rigidity, which is almost certainly also responsible for the slight displacement of the Fe out of the equatorial plane toward the MeCN ligand (by 0.09 Å).

Table 1. Selected Bond Lengths (Å) and Angles (deg) for $[FeL_1CH_3CN][FeCl_4]$ and $[MnL_1Cl][PF_6]$

	M = Fe	M = Mn
M−N(1)	2.089(6)	2.149(4)
M−N(2)	2.069(6)	2.267(4)
M−N(3)	1.906(6)	2.303(3)
M−N(4)	2.062(6)	2.268(4)
M−N(5)	1.889(6)	2.131(4)
M−N(6)	1.942(7)	
M−Cl(1)		2.454(2)
N(1)−M−N(2)	97.4(3)	100.14(14)
N(1)−M−N(3)	96.0(2)	92.41(13)
N(1)−M−N(4)	96.4(2)	97.80(14)
N(1)−M−N(5)	177.3(2)	169.66(14)
N(2)−M−N(3)	83.0(2)	73.64(12)
N(2)−M−N(4)	161.3(2)	142.48(13)
N(2)−M−N(5)	83.4(3)	77.66(14)
N(3)−M−N(4)	83.0(2)	72.93(13)
N(3)−M−N(5)	86.6(2)	77.27(14)
N(4)−M−N(5)	83.4(2)	78.82(14)
N(1)−M−N(6)/Cl(1)	89.4(2)	98.45(11)
N(2)−M−N(6)/Cl(1)	97.1(2)	103.86(10)
N(3)−M−N(6)/Cl(1)	174.5(3)	169.13(10)
N(4)−M−N(6)/Cl(1)	95.6(2)	105.73(10)
N(5)−M−N(6)/Cl(1)	87.9(3)	91.87(11)

Comparison of the structures (Figure 5a,b) shows that complexation with Mn causes significant changes in the ligand conformation. The most obvious effect is on the M−N distances. These increase substantially, though not by quite as much as would be expected for the replacement of low spin iron(II) by high spin manganese(II) (radii 0.75 and 0.97 Å, respectively).[13] The M−N(sp^3) distances have a rather larger spread than in

(10) Bryan, P. S.; Dabrowiak, J. C. *Inorg. Chem.* **1975**, *14*, 296.
(11) Riley, D. P.; Merrell, P. H.; Busch, D. H. *Inorg. Chem.* **1975**, *14*, 490.
(12) Lubben, M.; Meetsma, A.; Wilkinson, E. C.; Feringa, B.; Que, L., Jr. *Angew. Chem., Int. Ed. Engl.* **1995**, *34*, 1512.
(13) Shannon, R. D. *Acta Crystallogr.* **1976**, *A32*, 751.

Table 2. Electrochemical Data for the Complexes (V versus SHE in MeCN with 0.1 M Tetrabutylammonium Hexafluorophosphate)

$FeL_1(H_2O)(BF_4)_2$,	FeL_1SCN_2	$MnL_1Cl(PF_6)$	$MnL_1(CF_3SO_3)_2$
$E_{1/2} = 0.91$	$E_{1/2} = 0.53$	$E_{1/2} = 0.37$	$E_{1/2} = 0.84$
$E = 0.060$	$E = 0.075$	$E = 0.080$	$E = 0.22$
$E_a = 1.575$	$E_a = 0.77$		$E_{1/2} = 1.28$
			$E = 0.12$

the iron complex (2.149−2.268 Å), and the equatorial Mn−N(py) is slightly shorter (2.131 Å). However, the axial Mn−N(py) is considerably lengthened, to 2.303 Å, by a combination of the increased ion size and, possibly, the *trans*-influence of the chloride ion.

The lengthening of Mn−N(3) coupled with the rigidity of the ligand causes considerable distortions. The Mn ion is forced out-of-plane away from N(3) (0.39 Å from the equatorial N plane), and both pyridine rings are tipped away from the Mn−N directions (Mn−N···C angles of 159.3−159.8, compared to 174.1−174.6 (M = Fe)). Precisely similar distortions linked to increasing metal size and leading to substantial complex deformations have recently been noted in other complexes with dangling pyridine ligands.[14] They illustrate the significant structural effects that can be produced by the combination of a rigid ligand framework and an oversized metal ion.

Electrochemistry. Table 2 contains the electrochemical data for the complexes in acetonitrile. The almost reversible iron(III/II) couple for $[Fe(L_1)NCS]^+$ is observed at a modest value of 0.53 V vs SHE, in keeping with a mixture of ligands with preferences for either high or low oxidation states; the pyridines favor the divalent state while the bound anion and the relatively hard tertiary nitrogens favor the trivalent state. The second irreversible oxidation may involve the coordinated thiocyanate. In $[Fe(L_1)(H_2O)]^{2+}$, replacement of the thiocyanate by coordinated water destabilizes the trivalent state with an accompanying increase in potential. From the conductance values discussed earlier for the complexes, the manganese complexes are also of two types, one having a neutral sixth ligand (MeCN) and the other with a coordinated anion (Cl^-) at the sixth coordination site. As expected, the presence of the anion lowers the oxidation potential of the complexes by stabilizing the trivalent state. No reduction processes were observed

ESR Characterization. As expected, the iron(II) complexes were found to be ESR silent. Surprisingly, the high spin manganese(II) complex $MnL_1Cl(PF_6)$ gave only poorly resolved spectra in a range of solvents when recorded as a frozen glass in liquid nitrogen. This was attributed to the poor quality of the glasses obtained. An ethanolic solution of $MnL_1(CF_3SO_3)_2$ produces a good quality glass enabling the determination of resolved ESR spectra. The spectrum exhibits six lines arising from the nuclear hyperfine interaction with the manganese nucleus ($I = {}^5/_2$). Splittings due to the nitrogen donors were not observed.

Reactions with *tert*-Butyl Hydroperoxide and Hydrogen Peroxide. In somewhat similar systems, oxidation of manganese(II) macrocycles by hydrogen peroxide has been reported to give higher valent species with oxo-dimer structures.[15] For comparison, oxidation of the three complexes $FeL_1(SCN)_2$, $MnL_1Cl(PF_6)$, and $MnL_1(CF_3SO_3)_2$ with both *tert*-butyl hydroperoxide and hydrogen peroxide was investigated. In either acetonitrile or acetone, all three complexes react with *tert*-butyl hydroperoxide to give an ESR signal as a frozen glass in liquid nitrogen consistent with an axially symmetric radical ($g = 2.029$ and $g = 2.008$) (Figure 6). No signals derived from metal-based species were detected. Similar radical species have been identified in iron porphyrin systems upon reaction with *tert*-butyl hydroperoxide. However, those complexes were found to be much less stable in the presence of *tert*-butyl peroxide than is true of the present case.[16] The identity of the radical was further probed through the use of the spin traps 5,5-dimethyl-1-pyrroline *N*-oxide (DMPO) and *N*-*tert*-butyl−phenyl-nitrone (PBN).[17] Both compounds form spin adducts with the radical, displaying four- and three-line ESR spectra, respectively, at room temperature. The results of computer simulation with the Public EPR Software Tools are consistent with the *tert*-butyl peroxyl spin adduct.

Using hydrogen peroxide as oxidant in acetonitrile led to large amounts of oxygen evolution and poorly resolved ESR spectra, often combined with small amounts of an organic precipitate that was not further characterized. Reactions in aqueous solutions similarly resulted in vigorous oxygen evolution. However, acetone solutions, after reaction with hydrogen peroxide, displayed an axially symmetric spectrum ($g = 2.01$ and $g = 2.00$) when recorded as frozen glasses cooled in liquid nitrogen. Spin adducts were identified with both DMPO and PBN, again showing four- and three-line spectra, respectively, at room temperature. Computer simulations supported these as the hydroperoxyl radical spin adducts. There remains some debate in the literature as to whether such spin adducts contain a hydroperoxyl or superoxide radical.[18,19]

This system is unusual in that neither high valent metal complexes nor peroxo complexes[20−24] have been detected. However, the abundant production of peroxyl or hydroperoxyl radicals is reminiscent of the anticancer drug Bleomycin.[23] The strong catalytic decomposition of hydrogen peroxide requires only the metal(III/II) couple in a radical-generating pathway, and our failure to observe metal-containing species may simply indicate that the metal exists predominantly in the divalent state at steady state.

In summary we have synthesized and characterized a rigid topologically constrained ligand, which forms stable complexes

(14) Rubak-Akimova, E. V.; Alcock, N. W.; Busch, D. H. *Inorg. Chem.* **1998**, *37*, 1563.
(15) (a) Koek, J. H.; Russell, S. W.; VanderWolf, L.; Hage, R.; Warner, J. B.; Spek, A. L.; Kerschner, J.; Delpizzo, L. *J. Chem. Soc., Dalton Trans.* **1996**, 353. (b) Larson, Me.; Lah, M. S.; Li, X.; Bonadies, J. A.; Pecoraro, V. L. *Inorg. Chem.* **1992**, *31*, 373. (c) Sakiyama, H.; Okawa, H.; Isobe, R. J. *Chem. Soc., Chem. Commun*. **1993**, 882. (d) Higuchi, C.; Hakiyama, H.; Okawa, H.; Isobe, R.; Fenton, D. E. *J. Chem. Soc., Dalton Trans*. **1994**, 1097. Larson, E. J.; Pecoraro, V. L. *J. Am. Chem. Soc*. **1991**, *113*, 3810.
(16) Tajima, K.; Jinno, J.; Ishizu, K.; Sakurai, H.; Ohya-Nishiguchi, H. *Inorg. Chem.* **1989**, *28*, 709.
(17) (a) Evans, C. A. *Aldrichimica Acta* **1979**, *12*, 23. (b) Janzen, E. G. In *Free Radicals in Biology*; Pryor, W. A., Ed.; Academic Press; New York, 1979; Vol. IV, p 115. (c) Janzen, E. G.; Haire, D. L. *Adv. Free Radical Chem.* **1990**, *1*, 253.
(18) Finkelstein, E.; Rosen, G. M.; Raukman, E. J. *J. Am. Chem. Soc.* **1980**, *102*, 4994.
(19) Harbour, J. R.; Hair, M. L. *J. Phys. Chem.* **1978**, *82*, 1397.
(20) Walling, C. *Acc. Chem. Res.* **1975**, *8*, 125.
(21) Blum, R. H.; Carter, S. K.; Agre, K. A. *Cancer* **1973**, *31*, 903.
(22) (a) Hecht, S. M. Acc. *Chem. Res.* **1986**, *19*, 383. (b) Stubbe, J.; Kozarich, J. W. *Chem. Rev.* **1987**, *87*, 1107.
(23) (a) Sam, J. W.; Tang, X.-J.; Peisach, J. *J. Am. Chem. Soc*. **1994**, *116*, 5250. (b) Westre, T. E.; Loeb, K. E.; Zaleski, J. M.; Hedman, B.; Hodgson, K. O.; Solomon, E. I. *J. Am. Chem. Soc.* **1995**, *117*, 1309.
(24) (a) Sauer-Masarwa, A.; Herron, N.; Fendrick, C. M.: Busch, D. H. *Inorg. Chem.* **1993**, *32*, 1086. (b) Guajardo, R. J.; Hudson, S. E.; Brown, S. J.; Mascharak, P. K. *J. Am. Chem. Soc*. **1993**, *115*, 9524. (c) Kim, J.; Larka, E.; Wilkinson, E. C.; Que, L., Jr. *Angew. Chem., Int. Ed. Engl*. **1995**, *34*, 2048. (d) Bernal, I.; Jensen, I. M.; Jensen, K. B.; McKenzie, C. J.; Toftlund, H.; Tuchagues, J.-P. *J. Chem. Soc., Dalton Trans*. **1995**, 3667. (e) de Vries, M. E.; La Crois, R. M.; Roelfes, G.; Kooijman, H.; Spek, A. L.; Hage, R.; Feringa, B. L. *Chem. Commun. (Cambridge)* **1997**, 1549.

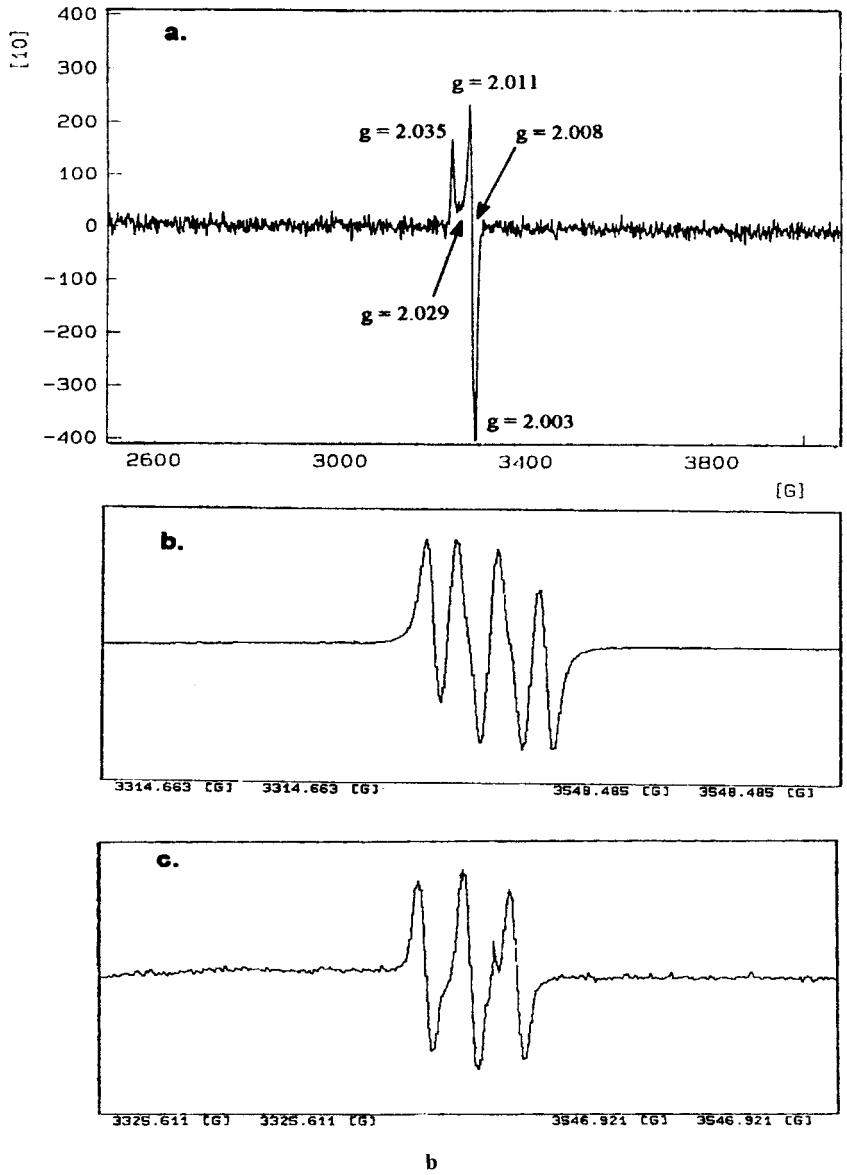

b

Figure 6. ESR spectra of products from reaction of $FeL_1(NCS)_2$ with *t*-BuOOH in acetone media: (a) reaction products frozen in acetone glass at 77 K; (b) reaction products + DMPO at 298 K; (c) reaction products + PBN at 298 K.

with both iron(II) and manganese(II) ions. The complexes demonstrate a high degree of stability with respect to ligand dissociation in acidic solution. Attempts at oxidizing these complexes with *tert*-butyl hydroperoxide and hydrogen peroxide produce the *tert*-butyl peroxyl and hydroperoxyl radicals, respectively. These results recall the recurrent proposal that metal hydroperoxyl species can be viable alternatives to high-valent metal−oxo species in catalytic or even enzymatic oxidation mechanisms.

Experimental Section

Materials. Solvents and reagents were of the highest grade available and were found to be sufficiently pure for use as supplied. Where necessary, solvents were dried by standard procedures.

Physical Techniques. ^{1}H and ^{13}C NMR spectra were recorded with either a QE 300 Plus or a Bruker DRX400 spectrometer. IR spectra were recorded as KBr disks using a Perkin-Elmer 1600FTIR spectrometer. Electronic spectra were recorded using a Hewlett-Packard 84552 diode array spectrometer with an 89500 UV/vis Hewlett-Packard ChemStation. Mass spectra (fast atom bombardment) were obtained using a VG ZAB HS spectrometer equipped with a xenon gun; several matrixes were used, including NBA (nitrobenzyl alcohol) and TG/G (thioglycerol/glycerol).

ESR spectra were recorded on a Bruker ESP300E spectrometer operating in the X band. Spectra were mainly recorded as frozen glasses in liquid nitrogen. The spin-trapping experiments involved reaction mixtures composed of 2.5×10^{-7} mol of complex (250 mL of a 1 mM stock solution), 5×10^{-5} mol of either *tert*-butyl hydroperoxide or hydrogen peroxide, and 5×10^{-5} mol of the appropriate spin trap. The spin adduct spectra were recorded in capillaries at room temperature.

Electrochemical experiments were performed on a Princeton Applied Research model 175 programmer and model 173 potentiostat. The output was recorded on paper using a Houston Instruments recorder. A glassy carbon electrode, a silver wire, and a platinum wire were used as working, reference, and secondary electrodes, respectively. Under nitrogen, acetonitrile solutions of the complexes (1 mM) with tetrabutylammonium hexafluorophosphate (0.1 M) as a supporting electrolyte were used in the experiments. The potentials vs NHE were determined using ferrocene as either an internal or external reference.

Solution magnetic susceptibilities were determined by the Evans method[25] on a Varian AM500 NMR instrument. Several milligrams of the appropriate complex was dissolved in 0.5 mL of deuterated acetonitrile (containing 1% TMS) in an NMR tube. Then an inner tube

(25) (a) Evans, D. F. *J. Chem. Soc.* **1959**, 2003. (b) Sur, S. K. *J. Magn. Reson.* **1989**, *82*, 169.

with a narrow end containing the blank solvent was inserted into the solution containing the complex. The paramagnetic solute caused the resonance of the TMS peak to shift downfield compared to the sample in the inner tube. Diamagnetic corrections were made using Pascal's constants. Cryomagnetic studies used a *force magnetometer* in an external magnetic field of 5 kG, which has previously been described.[26] Samples were pumped for over 3 h at a vacuum of 50 mTorr before the sample chamber was filled with helium gas for the variable temperature measurements.

Synthesis of the Ligand 5-Methyl-1,5,9,24,25-pentaazapentacyclo-[7.7.7.5.5]pentacosane-11,13,15,18(25),20,22-hexene (L_1). The macrocycle 7-methyl-3,7,11,17-tetraazabicyclo[11.3.1]heptadecane-1(17),13,15-triene (L_2) was synthesized by a literature procedure.[27] Similarly the reaction of 2,6-pyridinedimethanol with methanesulfonyl chloride was performed by a literature procedure.[28]

7-Methyl-3,7,11,17-tetraazabicyclo[11.3.1]heptadecane-1(17),13,15-triene (1.49 g, 6 mmol) and O,O′-bis(methanesulfonate)-2,6-pyridine dimethanol (1.77 g, 6 mmol) were separately dissolved in acetonitrile (60 mL). They were then added via a syringe pump (at a rate of 1.2 mL/h) to a suspension of anhydrous sodium carbonate (53 g, 0.5 mol) in acetonitrile (1380 mL). The temperature of the reaction mixture was maintained at 65 °C throughout the total reaction time of 60 h.

After cooling the solvent was removed under reduced pressure and the residue was dissolved in sodium hydroxide solution (200 mL, 4 M). The product was then extracted with benzene (6 × 100 mL), and the combined organic extracts were dried over anhydrous sodium sulfate. After filtration the solvent was removed under reduced pressure. The product was then dissolved in an acetonitrile/triethylamine mixture (95:5) and was passed through a column of neutral alumina (2.5 × 12 cm). Removal of the solvent yielded a white solid (0.93 g, 44%).

This product may be further purified by recrystallization from an ethanol/diethyl ether mixture combined with cooling at 0 °C overnight to yield a white crystalline solid. Anal. Calcd for $C_{21}H_{29}N_5$: C, 71.75; H, 8.32; N, 19.93. Found: C, 71.41; H, 8.00; N, 20.00. A mass spectrum displayed the expected molecular ion peak (for $[C_{21}H_{30}N_5]^+$) at m/z = 352. The ^{1}H NMR (400 MHz, in CD_3CN) spectrum exhibited peaks at δ =1.81 (m, 4H), 2.19 (s, 3H), 2.56 (t, 4H), 3.52 (t, 4H), 3.68 (AB, 4H), 4.13 (AB, 4H), 6.53 (d, 4H), and 7.07 (t, 2H). The ^{13}C NMR (75.6 MHz, in CD_3CN) spectrum showed eight peaks at δ = 24.05, 58.52, 60.95, 62.94, 121.5, 137.44 and 159.33. Crystals suitable for study by X-ray diffraction were obtained by cooling an acetonitrile solution of the ligand in a freezer overnight, though these proved to an adventitiously formed chloride salt.

Complexation Reactions. All metal complexation reactions were performed in a dry nitrogen filled Vacuum Atmospheres Corp. (VAC) glovebox, equipped with a gas circulation and oxygen removal system (VAC M040-1 dry train). Oxygen concentrations were maintained at or below 1 ppm.

Synthesis of $FeL_1(H_2O)(BF_4)_2$. Bis(pyridine)iron(II) chloride was prepared according to a literature procedure.[29] The ligand L_1 (0.833 g, 2.5 mmol), sodium tetrafluoroborate (0.55 g, 5 mmol), and triethylamine (0.505 g, 5 mmol) were dissolved in acetonitrile (5 mL). To this was added bis(pyridine)iron(II) chloride to yield a dark red solution, which was stirred for 1 h. The solvent was then removed under reduced pressure, and the resulting solid was dissolved in methanol and after removal from the glovebox was cooled in a freezer overnight to produce dark red microcrystals. Yield: 0.52 g (35%). Anal. Calcd for $Fe_1C_{21}H_{31}N_5O_1B_2F_8$: C, 42.06; H, 5.21; N, 11.68. Found: C 42.31; H, 5.37; N, 11.23. A mass spectrum displayed the molecular ion peak (for $[Fe_1C_{21}H_{29}N_5F_1]^+$) at m/z = 426.The IR spectrum (KBr) of the spectrum showed peaks at 1611 and 1578 cm^{-1} (pyridine) and a strong peak at 1083 cm^{-1} (BF_4^-). The electronic spectra of a dilute solution in acetonitrile exhibited a band at 400 nm (ϵ = 1981 M^{-1} cm^{-1}).

Synthesis of $FeL_1(SCN)_2$. Iron(II) trifluoromethanesulfonate was prepared in situ according to a literature procedure.[30] The ligand L_1 (0.833 g, 2.5 mmol) and triethylamine (0.505 g, 5 mmol) were dissolved in acetonitrile (5 mL). To this was added a solution of hexakis-(acetonitrile)iron(II) trifluoromethanesulfonate (1.5 g, 2.5 mmol) in acetonitrile (5 mL) to yield a dark red solution. Sodium thiocyanate (0.406 g, 5 mmol) was then added and the reaction mixture stirred for an additional 1 h. The solvent was then removed under reduced pressure, and the resulting solid was recrystallized from methanol to produce red microcrystals. Yield: 0.65 g (50%). Anal. Calcd for $Fe_1C_{23}H_{29}N_7S_2$: C, 52.76; H, 5.59; N, 18.74. Found: C 52.96; H, 5.53; N, 18.55. A mass spectrum displayed the expected molecular ion peak (for $[Fe_1C_{22}H_{29}N_6S_1]^+$) at m/z = 465. ^{1}H NMR (300 MHz, CD_3CN): δ = 1.70 (AB,2H), 2.0 (AB, 2H), 2.24 (s, 3H), 2.39 (m, 2H), 2.70 (m, 4H), 3.68 (m, 4H), 3.95 (m, 4H), 4.2(AB, 2H), 7.09 (d,2H), 7.19 (d, 2H), 7.52 (t, 1H), 7.61 (d, 1H). ^{13}C NMR (75 MHz, CD_3CN): 22.23, 58.80, 63.79, 66.33, 72.76, 119.06, 119.33, 135.86, 136.22, 163.01, 163.31. The IR spectrum (KBr) showed peaks at 1608 cm^{-1} (pyridine) and strong peaks at 2099 and 2037 cm^{-1} (SCN^-). The electronic spectra of a dilute solution in water exhibited a band at 388 nm, with a shoulder at 450 nm (ϵ = 1328 and 1097 M^{-1} cm^{-1}, respectively).

Synthesis of $FeL_1CH_3CN(FeCl_4)$. Iron(II) trifluoromethanesulfonate was prepared in situ as above. The ligand L_1 (0.833 g, 2.5 mmol) was dissolved in acetonitrile (5 mL). To this was added a solution of hexakis(acetonitrile)iron(II) trifluoromethanesulfonate (1.5 g, 2.5 mmol) in acetonitrile (5 mL). After stirring for 1 h the solvent was removed under reduced pressure and the product recrystallized by slow evaporation of an ethanol solution, yielding crystals suitable for study by X-ray crystallography. Mass spectrum: FeL_1Cl^+ at m/z = 442. Anal. Calcd for $Fe_2C_{22}H_{32}N_6Cl_4$: C, 43.47; H, 5.55; N, 12.18. Found: C, 42.17; H, 6.00; N, 11.98.

Synthesis of $MnL_1Cl(PF_6)$. Bis(pyridine)manganese(II) chloride was synthesized according to a literature procedure.[31] The ligand L_1 (1.24 g, 3.5 mmol), triethylamine(0.35 g, 3.5 mmol), and sodium hexafluorophosphate (0.588 g, 3.5 mmol) were dissolved in pyridine (12 mL). To this was added bis(pyridine)manganese(II) chloride, and the reaction mixture was stirred overnight. The reaction mixture was then filtered to remove a white solid. This solid was washed with acetonitrile until the washings were no longer colored, and then the combined organic filtrates were evaporated under reduced pressure. The residue was dissolved in the minimum amount of acetonitrile and allowed to evaporate overnight to produce bright red crystals suitable for study by X-ray crystallography. Yield: 0.8 g (39%). Anal. Calcd for $C_{21}H_{31}N_5$-$Mn_1Cl_1P_1F_6$: C, 43.00; H, 4.99; N, 11.95. Found: C, 42.88; H, 4.80; N, 11.86. A mass spectrum displayed the expected molecular ion peak (for $[C_{21}H_{31}N_5Mn_1Cl_1]^+$) at m/z = 441. The electronic spectrum of a dilute solution in water exhibited two absorption bands at 260 and 414 nm (ϵ = 10417 and 408 M^{-1} cm^{-1}, respectively). The IR spectrum (KBr) of the complex showed a band at 1600 cm^{-1} (pyridine) and strong bands at 840 and 558 cm^{-1} (PF_6^-).

Synthesis of $MnL_1(CF_3SO_3)_2$. Manganese(II) trifluoromethanesulfonate was prepared in situ according to a literature procedure,[9] and 0.883 g (2.5 mmol) was dissolved in acetonitrile (5 mL). This was added to a solution of the ligand L_1 (0.878 g, 2.5 mmol) and triethylamine (0.25 g, 2.5 mmol) in acetonitrile (5 mL). This was then heated for 2 h, filtered, and cooled, followed by removal of the solvent under reduced pressure. The residue was dissolved in a minimum amount of acetonitrile and left to evaporate slowly to yield orange crystals. Yield: 1.06 g (60%). Anal. Calcd for $Mn_1C_{23}H_{29}N_5S_2F_6O_6$: C, 39.20; H, 4.15; N, 9.95. Found: C, 38.83; H, 4.35; N, 10.10. The mass spectrum displayed the expected peak for $[Mn_1C_{22}H_{29}N_5S_1F_3O_3]^+$ at m/z = 555. The electronic spectrum of a dilute solution in water exhibited two absorption bands at 260 and 414 nm (ϵ = 9733 and 418 M^{-1} cm^{-1}, respectively). The IR spectrum (KBr) of the complex showed bands at 1600 cm^{-1} (pyridine) and 1260, 1160, and 1030 cm^{-1} (CF_3-SO_3).

(26) Kahol, P. K.; McCormick, B. J. *J. Phys. Condens. Matter* **1991**, *3*, 7963.
(27) Balakrishnan, K. P.; Omar, H. A. A.; Moore, P.; Alcock, N. W.; Pike, G. A. *J. Chem. Soc., Dalton Trans.* **1990**, 2965.
(28) Crossland, R. K.; Servis, K. L. *J. Org. Chem.* **1970**, *35*, 3195.
(29) Long, G. J.; Whitney, D. L.; Kennedy, J. E. *Inorg. Chem.* **1971**, *11*, 1406.
(30) Tait, A. M.; Busch, D. H. *Inorg. Synth*. **1978**, *XVIII*, 7.
(31) Witteveen, H. T.; Nieuwenhuijse, B.; Reedijk, J. *J. Inorg. Nucl. Chem.* **1974**, *36*, 1535.

Table 3. Crystal Data

	HL_1ClH_{20}	$[FeL_1CH_3CN][FeCl_4]EtOH$	$[MnL_1Cl][PF_6]$
empirical formula	$C_{21}H_{32}ClN_5O$	$C_{25}H_{38}N_6OFe_2Cl_4$	$C_{21}H_{29}N_5ClMnPF_6$
fw	403.95	692.11	586.85
temp/K	180(2)	230(2)	293(2)
cryst syst	orthorhombic	monoclinic	monoclinic
space group	$P2_12_12_1$	$P2_1/n$	$P2_1/n$
a/Å	9.4405(5)	10.0460 (5)	7.745(2)
b/Å	13.3617(5)	19.237(9)	22.786(4),
c/Å	16.710(1)	15.6254(8)	14.639(4)
β	90	95.97(2)	105.074(10)
vol/Å^3, *Z*	2107.82(4), 4	3002.7(3), 4	2494.3(10), 4
Cell-determining reflns	8732	3494	5242
D(calcd)/Mg/m^3	1.273	1.531	1.563
F(000)	864	1432	1204.
(Mo Kα)/mm^{-1}	0.203	1.353	0.766
crystl dimens/mm	0.60 × 0.40 × 0.30	0.22 × 0.20 × 0.10	0.23 × 0.23 × 0.23
θ_{max}/deg	28.56	23.25	25
hkl ranges	−12/10, −17/16, −21/21	−11/9, −18/21, −17/16	−9/3, −30/28, −18/17
reflns total	12952	13125	9878
unique, *R*(int)	4835, 0.027	4307	4307, 0.048
With $I > 2(I)$	4264	2783	3311
transm factors	0.84, 0.96	correction not applied	correction not applied
params	266	344	316
weighting params *a*, *b*	0.0294, 0.5516	0.026, 12.8	0.0457, 5.85
largest *F* peaks/e·Å^{-3}	0.187, −0.245.	0.52, −0.43	0.684, −0.441
goodness-of-fit (F^2)	1.085,	1.156	1.072
R1[$I > 2\sigma(I)$]	0.037	0.068	0.062
wR2 (all reflns)	0.083	0.146	0.152

X-ray Structure Determination. Crystal and refinement data are given in Table 3. A Siemens SMART three-circle system was used with CCD area detector,[32] and Mo Kα radiation (λ 0.71073 Å). Cell parameters were determined by least-squares fitting to numerous reflection positions. Temperature control was with the Oxford Cryosystem Cryostream Cooler.[33] Absorption correction was by ψ-scan for L_1 only; crystal decay was checked by repeating the initial frames at the end of the collection; none of the crystals showed any decay.

Structure Analysis and Refinement. For all three compounds, the systematic absences indicated the space groups uniquely. The structures were solved by direct methods using SHELXS (TREF) with additional light atoms found by Fourier methods.[34] Hydrogen atoms were added at calculated positions and refined using a riding model with freely rotating methyl groups. Anisotropic displacement parameters were used for all non-H atoms; H atoms were given isotropic displacement parameters equal to 1.2 (or 1.5 for methyl hydrogen atoms) times the equivalent isotropic displacement parameter of the atom to which the H atom is attached. Refinement was on F^2 (all reflections) using SHELXL 96.[35] The weighting scheme was calc $w = 1/[\sigma^2(F_o^2) + (aP)^2 + bP]$ where $P = (F_o^2 + 2F_c^2)/3$.

For L_1 the asymmetric unit contains one molecule of water; the absolute structure of the individual crystal chosen was checked by refinement of a $\Delta f''$ multiplier; absolute structure parameter $x = 0.03(5)$. For FeL_1, the asymmetric unit contains one molecule of EtOH.

Acknowledgment. This research was generously supported by a grant from the Procter and Gamble Company. We thank EPSRC and Siemens Analytical Instruments for grants in support of the diffractometer. The Warwick−Kansas collaboration has been facilitated by NATO support.

Supporting Information Available: Tables of atomic coordinates, thermal parameters, and full bond lengths and angles. This material is available free of charge via the Internet at http://pubs.acs.org.

IC981410F

(32) *SMART User's manual*; Siemens Industrial Automation Inc.: Madison, WI, 1994.
(33) Cosier, J.; Glazer, A. M. *J. Appl. Crystallogr.* **1986**, *19*, 105.
(34) Sheldrick, G. M. *Acta Crystallogr.* **1990**, *A46*, 467.
(35) Sheldrick, G. M. SHELX-96 (beta-test) (including SHELXS and SHELXL), University of Göttingen, 1996.